Aust. J. Phys., 1981, 34, 333–55

A Southern Survey of OH Masers at 1612 MHz

J. L. Caswell,[A] R. F. Haynes,[A] W. M. Goss[A,B] and U. Mebold[A,C]

[A] Division of Radiophysics, CSIRO, P.O. Box 76, Epping, N.S.W. 2121.
[B] Present address: Sterrenkundig Laboratorium Kapteyn, Hoogbouw WSN, University of Groningen, Postbus 800, Groningen, Netherlands.
[C] Present address: Max Planck Institut für Radioastronomie, Auf dem Hügel 69, D-5300 Bonn 1, West Germany.

Abstract

A search for OH at 1612 MHz has been made along the galactic plane from longitude 340° to the galactic centre, yielding 78 emission sources (mostly new discoveries); a further 5 sources have been found in a less sensitive survey between longitudes 270° and 326°. Of these 83 sources 55 are masers of the variety showing two intensity peaks spaced in velocity—a characteristic of OH/IR stars. The velocity and spatial distributions of these new OH/IR stars (which are not as yet identified in the optical or infrared) are discussed, with special reference to their kinematic properties and population type; it is still not clear whether they are predominantly late-type giants (Mira variables) or supergiants. The other 28 OH sources detected include 11 of the type IIc variety (extended OH clouds exhibiting 1612 MHz emission with accompanying 1720 MHz absorption) and 4 with accompanying main-line (type I) OH masers; the remaining 13 sources do not readily fit within existing classification schemes and are discussed individually.

1. Introduction

Several surveys of 1612 MHz OH emission in the plane of the Galaxy have recently been reported (Caswell and Haynes 1975; Johansson *et al.* 1977*a*; Bowers 1978*a*; Baud *et al.* 1979*a*, 1979*b*). Most of the 1612 MHz OH sources discovered are double-peaked in velocity and show negligible polarization while emission on the 1665 or 1667 MHz lines is generally weak or absent and the 1720 MHz line is never detectable. These properties are characteristic of OH emission from the circumstellar shells of late-type stars and the OH sources are a valuable stellar probe, especially in directions where optical obscuration is severe.

Early surveys concentrated on galactic longitude ranges 326°–340° and 12°–234°, and thus specifically excluded the galactic centre region. The results of these surveys made it clear that a search extending to the galactic centre would be valuable; consequently our present survey was chosen to cover the longitude range 340°–2° while the more northerly region 358°–14° was recently covered by Baud *et al.* (1979*a*).

2. Observations

(*a*) General

All observations were made with a dual-channel 18 cm parametric amplifier installed on the Parkes 64 m paraboloid; the system temperature of each channel was ~80 K on cold regions of sky. Two orthogonal linear polarizations were sampled and with appropriate phasing were combined at IF to yield the two senses (RH and LH) of circular polarization. The spectral line analysis was performed with the 1024 channel digital autocorrelator, yielding a 512 point spectrum for each circular polarization simultaneously.

The intensity calibration is relative to Hydra A, for which a total flux density of 36 Jy was assumed (18 Jy in each sense of circular polarization); the beam size to half-power is $12'\cdot6$ arc at 1612 MHz and the ratio of flux density to antenna temperature for *each* polarization is $0\cdot8$ Jy K^{-1}.

(*b*) *Initial Survey for New Sources*: *1976 March and July*

(i) *Longitude range 340°–355°.* Positions at $b = 0°$ and $\pm0°\cdot2$, and spaced $0°\cdot2$ in longitude were observed. Observations at $|b| \geqslant 0°\cdot4$ were made where sources were detected at the edge of the original grid. The spectrum bandwidth analysed was 2 MHz and covered the velocity range -230 to $+130$ km s^{-1}. The resolution (with uniform weighting) was $4\cdot8$ kHz ($\equiv 0\cdot8$ km s^{-1}). Integrations for 7 min at each grid position were combined with a 15 min reference to yield an r.m.s. noise level (in directions with no strong continuum radio emission) of $0\cdot1$ K ($\equiv 0\cdot08$ Jy) in each sense of polarization.

(ii) *Longitude range 355°–2°.* Nearer the galactic centre we anticipated that the velocity range of any detectable emission might be somewhat larger, and in this region a bandwidth of 5 MHz was observed giving a velocity coverage of -450 to $+450$ km s^{-1} and a resolution, with uniform weighting, of 12 kHz. The grid spacing in longitude was $0°\cdot2$ and for longitudes 355° to 358° the latitudes observed were $b = 0°$, $\pm0°\cdot2$ and $\pm0°\cdot4$; we also observed from $l = 358°\cdot2$ to $+2°$ (but only at $b = 0°$) in order to provide a small comparison region with the Baud *et al.* (1979*a*) survey.

(iii) *Longitude range 270°–326°.* A fast survey (integration time 2 min at each grid point), limited to $b = 0°$ with grid points spaced $0°\cdot2$ in longitude, was made in this region. Four new double-peaked OH/IR stars were detected and a new position measurement of OH $305\cdot91-1\cdot91$ was made.

(*c*) *Further Study*: *1977 March and September, 1978 August*

An accurate position was measured for each source, using a grid with $6'$ arc spacing centred on the preliminary estimate of the source position. Observations were then made at the source position with higher frequency resolution; a $0\cdot5$ MHz total bandwidth was generally used for the stronger sources, yielding a velocity coverage of 90 km s^{-1} and a resolution of 2 kHz (after Hanning weighting). For sources which were circularly polarized at 1612 MHz, additional observations on the main-line transitions (1665 and 1667 MHz) were made and for those sources showing only a single velocity feature at 1612 MHz further observations were made at 1720 MHz.

3. Results

(*a*) *OH Emission Sources*: *Tabulation and Figures*

In Table 1 we list the 83 emission sources detected in the survey. The measured positions are given in columns 1–5. The galactic coordinates of columns 1 and 2 together with the prefix 'OH' are subsequently used as the source names. The radial velocities and peak total intensities are summarized in columns 6 and 7, and the epoch of measurement is given in column 8. In many cases a figure is shown (see column 9) and should be referred to for more details of the emission. The source type is given in column 10 (see below for a description of the designations used) and for some sources (in particular those which cannot readily be classified) reference is made to notes in the text (Section 3*b*) and to earlier publications in the case of four previously known sources. For double-peaked (OH/IR) sources the separation in velocity and the mean velocity are given (columns 11 and 12). A kinematic distance is given in column 13 (calculated from the mean velocity; see Section 4*a*). With the adoption of these distances an 'intrinsic luminosity' is given for OH/IR sources in column 14; it is the intensity of the strongest peak if the source had been situated at a distance of 1 kpc.

Note that OH 344·83−1·67 and OH 345·05−1·86 fall outside the intended survey limits and were discovered by accident while doing a reference integration. OH 305·91−1·91 also lies outside the survey area and was observed to measure an improved position.

Apart from a few miscellaneous sources, most of the sources fit into three known classes as follows.

(i) *Type II OH/IR stars.* These have intensity peaks at two velocities separated typically by 20–50 $\mathrm{km\,s^{-1}}$; in general we have relied wholly on the 1612 MHz OH appearance, together with the absence of circular polarization, to classify these sources.

(ii) *Type I sources.* These are associated with main-line emission having an intensity comparable with or exceeding the 1612 MHz emission. The main-line emission is generally circularly polarized and in some cases the 1612 MHz emission also shows considerable circular polarization.

(iii) *Type IIc.* These are weak unpolarized single broad-velocity features and are probably spatially extended; in many cases our measurements at 1720 MHz show absorption, as is common for these sources (see Caswell and Haynes 1975).

(*b*) *Notes on Some Individual Sources*

OH305·91−1·91. Discovered by Bowers and Kerr (1978); outside our survey area but observed in order to measure a more accurate position.

OH339·93+0·37 (Fig. 1). Single feature, showing some circular polarization. Intensity decreased between 1977 September and 1978 August. High negative velocity suggests it is near tangent point. Not detected at 1665, 1667 or 1720 MHz.

OH340·00−0·51 and OH340·14−0·45 (Fig. 1). Each profile shows emission from the other source, somewhat attenuated by the offset from the beam centre.

OH340·24−0·06 (Fig. 1). Single feature, quite narrow ($\sim$1 $\mathrm{km\,s^{-1}}$). No significant circular polarization. High velocity suggests it is near tangent point. Not detected at 1665, 1667 or 1720 MHz.

OH342·01+0·25 (Fig. 2). Single broad feature ($\sim$10 $\mathrm{km\,s^{-1}}$). Intensity may vary (apparently stronger in 1978 August than in 1977 March). Emission at 1667 MHz is present in the same direction but displaced in velocity to $v = -31$ $\mathrm{km\,s^{-1}}$. Not detected at 1665 or 1720 MHz.

OH342·2+0·2. Type IIc, showing 1720 MHz absorption at the same velocity as the 1612 MHz emission. Note that the high velocity indicates that the OH cloud is quite distant.

OH343·12−0·06 (Fig. 2). Type I source, with accompanying 1665 and 1667 MHz emission (unpublished data) and also H_2O maser emission (Batchelor *et al.* 1980).

Table 1. OH emission at 1612 MHz

(1) Galactic coordinates l °	(2) b °	(3) Position (1950) R.A. h m s	(4) Dec. ° ′ ″	(5) RMS error[A] ″	(6) Radial velocities (l.s.r.) (km s^{-1})		(7) Peak intensities (Jy)		(8) Date	(9) Fig. No.	(10) Source type and notes[B]	(11) Δv sepn (km s^{-1})	(12) Mean vel. (km s^{-1})	(13) Kinematic distance[C] (kpc)	(14) Intrinsic luminosity (Jy kpc^2)
285·05	+0·07	10 28 43·1	−57 34 16	35	−1	+35	1·6	2·2	77 Mar.	—	OH/IR	36	+17	7·2	114
286·50	+0·06	10 38 09·6	−58 17 48	35	+9	+41	2·1	2·3	77 Mar.	—	OH/IR	32	+25	8·3	158
300·93	−0·03	12 31 01·3	−62 33 43	45	+37	+60	2·9	0·9	77 Mar.	—	OH/IR	23	+48·5	14·0	568
305·91	−1·91	13 15 58·9	−64 21 44	30	−76	−46	1·8	1·3	76 Mar.	—	OH/IR; see text	30	−61	5·9	63
315·22	+0·01	14 29 45·0	−60 10 53	35	−99	−67	2·2	1·9	77 Apr.	—	OH/IR	32	−83	7·0	108
339·93	+0·37	16 41 31·3	−44 57 53	60	−116		2·1		77 Sept.	1	?; see text			9·4±0	
339·98	−0·19	16 44 04·3	−45 17 46	20	−44	−7	2·4	3·7	77 Mar.	1	OH/IR	37	−26·5	*2·5* or 16·3	23
340·00	−0·51	16 45 31·8	−45 29 18	10	−80	−35	2·4	3·6	77 Mar.	1	OH/IR; see text	45	−57·5	*4·9* or 13·9	86
340·14	−0·45	16 45 47·4	−45 20 21	25	−102	−72	2·4	2·1	77 Mar.	1	OH/IR; see text	30	−87	*6·9* or 11·9	114
340·24	−0·06	16 44 28·0	−45 00 54	60	−122		2·2		77 Sept.	1	?; see text			9·4±0	
340·42	−0·01	16 44 56·2	−44 51 01	20	−168	−135	3·4	2·6	77 Mar.	1	OH/IR	33	−151·8	9·4	300
340·82	+0·00	16 46 20·0	−44 32 02	25	−144	−116	1·8	1·5	77 Mar.	1	OH/IR	28	−130	9·4	159
341·12	−0·00	16 47 26·1	−44 18 25	25	−61	−25	2·1	1·9	77 Mar.	1	OH/IR	36	−43	*4·0* or 15·0	34
341·28	+0·12	16 47 30·1	−44 06 22	15	−32	−3	6·4	5·0	77 Mar.	2	OH/IR	29	−17·5	*1·8* or 17·1	21
342·01	+0·25	16 49 31·1	−43 27 40	15	−48		8·7		77 Mar.	2	?; see text			*4·5* or 14·5	
342·2	+0·2	16 50 24·7	−43 20 44	ext	−81		0·8		76 Mar.	—	IIc; see text			*6·7* or 12·3	
342·78	−0·08	16 53 36·0	−43 04 22	20	−127	−88	0·9	0·8	77 Sept.	2	OH/IR	39	−107·5	9·6±1·4	83
343·12	−0·06	16 54 43·2	−42 47 52	15	−28		28		77 Mar.	2	I; see text			*3·0* or 16·2	
343·38	+0·25	16 54 17·9	−42 23 55	60	−101	−73	1·0	1·3	77 Mar.	2	OH/IR	28	−87	9·6±2·5	120
343·8	−0·2	16 57 35·5	−42 21 06	ext?	−28		0·5		77 Mar.	—	IIc; see text			*3·1* or 16·1	
344·39	+0·03	16 58 35·0	−41 45 00	>30?	−67		1·4		77 Mar.	2	IIc?; see text			*6·2* or 13·0	
344·83	−1·67	17 07 17·5	−42 25 29	20	−71	−46	4·3	2·0	77 Mar.	2	OH/IR; see text	25	−58·5	*5·9* or 13·4	150
344·93	+0·01	17 00 25·8	−41 19 43	15	−23	+15	140	90	77 Mar.	2	OH/IR	38	−4	*0·5* or 18·7	35
345·05	−1·86	17 08 48·8	−42 21 47	15	−11	+18	26	20	77 Mar.	3	OH/IR; see text	29	+3·5	~*0* or 19·9	
345·70	−0·09	17 03 22·5	−40 47 02	10	−8						I; text; ref. 1			*1·1* or 18·3	

346·01+0·04	17 03 48·5	−40 27 17	20	−26	+9	2·0	2·4	77 Mar.	3	OH/IR	35	−8·5	*1·2* or 18·2	3
346·18+0·02	17 04 24·1	−40 19 50	~120	−39	−9	0·9	0·8	78 Aug.	3	OH/IR	30	−24	*3·0* or 16·5	8
346·86−0·18	17 07 23·2	−39 54 35	60	−31		1·4		77 Mar.	3	?; see text			*4·0* or 15·5	
347·09+0·21	17 06 30·9	−39 29 34	15	−150	−121	2·8	5·8	77 Mar.	3	OH/IR	29	−135·5	9·7±0	546
347·40+0·40	17 06 40·1	−39 08 11	15	−201	−176	11·4	10·2	77 Mar.	3	OH/IR	25	−188·5	9·7±0	1072
347·57+0·11	17 08 24·7	−39 10 02	25	−17	+2	0·8	1·4	77 Sept.	3	OH/IR	19	−7·5	*1·2* or 18·3	2
347·63+0·15	17 08 24·8	−39 05 50	10	−97						I; text; ref. 1			9·8±1·8	
349·18+0·20	17 12 51·6	−37 48 49	20	−26	+13	4·1	5·5	77 Mar.	3	OH/IR	39	−6·5	*1·2* or 18·5	8
349·36−0·20	17 15 01·9	−37 54 04	40	−126		0·6		77 Mar.	4	?; see text			9·8±0·8	
349·39−0·01	17 14 20·9	−37 45 40	35	+12	+38	0·8	0·7	78 Aug.	4	OH/IR	26	+25	*9·8* (or ~0)	77
349·50−0·52	17 16 47·3	−37 58 27	20	−91	−61	3·8	1·5	77 Mar.	4	OH/IR	30	−76	9·8±2·4	365
349·52+0·25	17 13 40·6	−37 30 29	20	+58	+86	3·5	0·8	77 Mar.	4	OH/IR	28	+72	*9·8* (or ~0)	336
349·6 +0·4	17 13 17·3	−37 21 27	ext?	−5		0·8		76 July	—	IIc; see text			*1·0* or 18·7	
349·81−0·32	17 16 49·9	−37 36 20	15	−18	+8	28	14	77 Mar.	4	OH/IR	26	−5	*1·0* or 18·7	28
349·96−0·03	17 16 04·7	−37 18 47	20	+39		6·0		77 Mar.	4	?; see text			*9·9* (or ~0)	
350·55+0·06	17 17 25·3	−36 46 57	25	−56	−27	6·1	2·0	77 Mar.	4	OH/IR	29	−41·5	*6·1* or 13·6	227
350·85+0·19	17 17 47·2	−36 27 49	15	−98	−73	12·5	10·6	77 Mar.	4	OH/IR	25	−85·5	9·9±1·8	1225
350·97+0·43	17 17 09·0	−36 13 18	35	−126	−99	1·7	1·2	77 Sept.	5	OH/IR	27	−112·5	9·9±1·2	167
351·14+0·08	17 19 04·2	−36 17 06	20	−109	−79	6·0	4·1	77 Mar.	5	OH/IR	30	−94	9·9±1·3	588
351·22+0·25	17 18 34·5	−36 07 03	60	−44	−18	1·7	0·8	77 Mar.	5	OH/IR	26	−31	*5·1* or 14·7	44
351·4 −0·4	17 21 44·2	−36 20 43	ext?	−21		0·8		76 July	—	IIc; see text			*3·9* or 15·9	
351·4 −0·6	17 22 33·3	−36 27 30	ext?	−36		0·6		76 July	—	IIc; see text			*5·9* or 13·9	
351·6 +0·2	17 19 51·3	−35 50 23	ext?	−39		0·6		77 Sept.	—	IIc; see text			*6·3* or 13·5	
351·6 −0·4	17 22 17·8	−36 10 49	ext?	−92		1·5		76 July	—	IIc; see text			9·9±1·5	
351·60+0·32	17 19 21·4	−35 46 32	35	+8	+28	2·0	1·1	77 Sept.	5	OH/IR	20	+18	~*0* (or 9·9)	?
351·75−0·53	17 23 15·2	−36 07 53	15?	−3		4·1		77 Sept.	5	IIc?; see text			*0·7* or 19·1	
352·61−0·19	17 24 13·7	−35 13 27	20	−29	+4	2·3	3·2	77 Mar.	5	OH/IR	33	−12·5	*2·9* or 17·0	27
353·15+0·09	17 24 36·0	−34 37 44	20	−83	−48	0·9	2·4	77 Sept.	5	OH/IR	35	−65·5	9·9±2·0	235
353·23−0·24	17 26 09·0	−34 44 37	60	+13		1·2		77 Sept.	5	?; see text			~*0* (or 10)	
353·41−0·36	17 27 05·2	−34 39 26	45	−16		1·7		77 Mar.	—	IIc; see text			*3·8* or 16·1	
353·60−0·23	17 27 06·7	−34 25 47	15	−102	−66	16·3	8·5	77 Mar.	6	OH/IR	36	−84	9·9±1·7	1598
354·53+0·03	17 28 32·1	−33 30 33	15	−52	−19	0·7	2·7	77 Sept.	6	OH/IR	33	−35·5	10·0±3·1	270
354·60+0·26	17 27 48·2	−33 19 46	25	−136	−107	1·6	2·1	77 Mar.	6	OH/IR	29	−121·5	10·0±1·0	210
354·62+0·47	17 27 01·1	−33 11 36	45	−15		2·0		77 Mar.	6	I; see text			*4·2* or 15·7	
354·75−0·06	17 29 29·3	−33 22 32	20	−13	+15	2·9	7·6	77 Mar.	6	OH/IR	28	+1	~*0* (or 10)	?

A,B,C See footnotes at end of table.

Table 1 (*Continued*)

(1) (2) Galactic coordinates l b ° °	(3) Position (1950) R.A. h m s	(4) Dec. ° ′ ″	(5) R.M.S. error[A] ″	(6) Radial velocities (l.s.r.) (km s^{-1})	(7) Peak intensities (Jy)	(8) Date	(9) Fig. No.	(10) Source type and notes[B]	(11) Δv sepn (km s^{-1})	(12) Mean vel. (km s^{-1})	(13) Kinematic distance[C] (kpc)	(14) Intrinsic luminosity (Jy kpc^2)
354·88−0·54	17 31 43·8	−33 31 41	15	−5 +24	116 322	77 Mar.	6	OH/IR; see text	29	+9·5	~*0* (or 10)	?
355·03+0·17	17 29 17·8	−33 01 07	35	+20	2·0	77 Mar.	6	?; see text			10·0	
355·38+0·08	17 30 35·3	−32 46 24	45	−190	1·0	77 Mar.	6	?; see text			10·0	
355·95−0·05	17 32 33·6	−32 21 40	20	−13	5·4	77 Mar.	7	?; see text			*4·7* or 15·3	
356·38+0·29	17 32 19·6	−31 48 59	25	+94 +121	1·4 1·6	77 Mar.	7	OH/IR	27	+107·5	10·0	160
356·46−0·38	17 35 11·4	−32 07 07	60	−138	0·8	77 Mar.	7	?; see text			10·0	
356·50−0·55	17 35 57·9	−32 10 20	15	+61 +86	14·5 54	78 Aug.	7	OH/IR; text; ref. 2	25	+73·5	10·0	5400
356·63−0·21	17 34 56·2	−31 53 03	60	−23 +3	1·9 0·8	77 Mar.	7	OH/IR	26	−10	*4·4* or 15·6	37
356·64−0·32	17 35 23·4	−31 55 36	60	−20	1·7	77 Mar.	7	?; see text			10·0±3·3	
357·0 +0·0	17 35 03·0	−31 27 23	ext?	−6	0·8	77 Sept.	—	IIc; see text			*3·2* or 16·7	
357·09−0·37	17 36 44·5	−31 34 36	20	+60 +82	3·6 2·1	77 Mar.	7	OH/IR	22	+71	10·0	360
357·18−0·52	17 37 35·0	−31 34 52	20	+19 +42	1·8 2·0	77 Sept.	7	OH/IR	23	+30·5	10·0	200
357·48+0·37	17 34 47·8	−30 51 11	20	+101 +129	4·1 3·7	77 Mar.	8	OH/IR	28	+115	10·0	410
357·68−0·06	17 37 00·9	−30 54 45	15	−253 −221	6·8 3·2	77 Mar.	8	OH/IR	32	−237	10·0	580
357·71−0·27	17 37 52·4	−31 00 11	25	−75 −44	3·3 1·4	77 Mar.	8	OH/IR	31	−59·5	10·0±1·1	330
357·75+0·34	17 35 36·9	−30 38 38	20	−106 −82	3·0 2·0	77 Mar.	8	OH/IR	24	−94	10·0	300
357·77−0·15	17 37 33·6	−30 53 25	30	−92 −68	2·0 2·2	77 Mar.	8	OH/IR	24	−80	10·0	220
358·16+0·50	17 35 59·2	−30 12 47	10	−18 +22	45 42	77 Mar.	8	OH/IR; text; ref. 3	40	+2	~*0* (or 10)	?
358·67−0·04	17 39 21·1	−30 04 19	45	−26 +27	4·6 1·0	78 Aug.	8	OH/IR; see text	53	+0·5	~*0* (or 10)	?
359·22+0·26	17 39 32·6	−29 26 44	20	−104	1·4	78 Aug.	—	?; see text			10·0	
359·22+0·18	17 39 51·2	−29 29 12	20	−150 −119	1·8 2·1	78 Aug.	9	OH/IR	31	−134·5	10·0	210
359·36+0·08	17 40 34·5	−29 25 03	20	−223 −199	1·7 4·5	78 Aug.	9	OH/IR	24	−211	10·0	450
1·48−0·06	17 46 11·1	−27 41 21	15	−141 −114	5·5 8·4	77 Mar.	9	OH/IR; see text	27	−127·5	10·0	840

[A] Sources which are probably extended are noted as 'ext' and the positional uncertainty is not known.
[B] References: ref. 1, Robinson *et al.* (1974); ref. 2, Hardebeck (1972); ref. 3, Allen *et al.* (1977).
[C] Preferred distance is printed in italics (see text).

Both 1665 and 1667 MHz emission are circularly polarized 100% LH but the 1612 MHz emission shows no significant polarization. No 1720 MHz emission is detectable.

OH 343·8−0·2. Type IIc, showing 1720 MHz absorption.

OH 344·39+0·03 (Fig. 2). Probably type IIc, with accompanying 1720 and 1667 MHz absorption. Caswell and Haynes (unpublished data) find a new 1665 MHz (type I) emission source in this direction.

OH 344·83−1·67 and OH 345·05−1·86 (Figs 2 and 3). OH/IR sources with galactic latitude outside the intended survey area; discovered while doing a reference integration.

OH 345·70−0·09. Type I OH maser with emission at 1612, 1665 and 1667 MHz (see Robinson *et al.* 1974; Caswell and Haynes 1975) and with an associated H_2O maser (Batchelor *et al.* 1980).

OH 346·86−0·18 (Fig. 3). Unusual type of source with a single peak of emission detected only at 1612 MHz; neither emission nor absorption detectable at 1720, 1667 or 1665 MHz.

OH 347·63+0·15. Type I OH maser with emission at 1612, 1665 and 1667 MHz (see Robinson *et al.* 1974). The position (Table 1) was obtained in the current observations. The source shows relatively strong excited state OH emission at 6035 MHz (Knowles *et al.* 1976).

OH 349·36−0·20 (Fig. 4). Unusual type of source: at 1612 MHz the emission is weak but circularly polarized; emission at 1667 MHz is present in this same direction, with comparable intensity and similar mean velocity but much broader ($\sim$20 km s^{-1}). The high negative velocity suggests that the source is quite distant.

OH 349·6+0·4. Type IIc showing 1720 MHz absorption.

OH 349·96−0·03 (Fig. 4). The 1612 MHz emission is a quite strong single feature but nothing was detected at 1665, 1667 or 1720 MHz. Note the quite large positive velocity.

OH 351·4−0·4. Type IIc, showing 1720 MHz absorption.

OH 351·4−0·6 and OH 351·6+0·2. Type IIc with similar velocities and thus probably close in space. Both show 1720 MHz absorption.

OH 351·6−0·4. Type IIc with 1720 MHz absorption; quite large velocity suggests source is quite distant. Caswell and Haynes (unpublished data) have discovered a new type I (1665 MHz) OH maser nearby.

OH 351·75−0·53 (Fig. 5). The broad (in velocity) 1612 MHz emission appears to be predominantly type IIc, with 1720 MHz absorption prominent in this direction. However, Caswell and Haynes (unpublished data) have discovered a new type I (1665 MHz) OH maser nearby ($<1'$ arc from the 1612 MHz position). The presence of some circular polarization in the 1612 MHz emission suggests that part of the 1612 MHz emission arises in compact knots associated with the type I source.

OH 353·23−0·24 (Fig. 5). Single feature at 1612 MHz and nothing detected at 1720 MHz. Type not clear.

OH 353·41−0·36. Type IIc with accompanying 1720 MHz absorption. In approximately the same direction is a type I OH maser (Caswell and Robinson 1974) showing 1665 MHz emission and an H_2O maser (Batchelor *et al.* 1980).

OH 354·62+0·47 (Fig. 6). New type I source, showing emission at 1612, 1665 and 1667 MHz, but none at 1720 MHz. The emission is 100% RH polarized on all three transitions.

OH354·88−0·54 (*Fig. 6*). OH/IR, the strongest detected in this survey and indeed one of the strongest known to date.

OH355·03+0·17 (*Fig. 6*). 1612 MHz emission is accompanied by weak broad (in velocity) 1667 MHz emission and even weaker 1665 MHz emission, with nothing detected at 1720 MHz. Type of source not clear.

OH355·38+0·08 (*Fig. 6*). Quite weak emission at 1612 MHz and nothing detected at 1665, 1667 or 1720 MHz; type of source unknown. Note the high velocity.

OH355·95−0·05 (*Fig. 7*). Quite strong emission at 1612 MHz and nothing detected at 1665, 1667 or 1720 MHz; type of source unknown.

OH356·46−0·38 (*Fig. 7*). Several weak emission features are present at 1612 MHz, spread over $\sim 20\ \mathrm{km\,s^{-1}}$ and with a high mean negative velocity. Nothing detected at 1665, 1667 or 1720 MHz. Note that the IR source IRC−30305 is at R.A. $17^h 34^m 55^s$, Dec. $-32° 07'·4$ and might be associated—improved positions of both the OH emission and IR source are needed to check this possibility.

OH356·50−0·55 (*Fig. 7*). OH/IR star first reported by Hardebeck (1972), who called the source OH 1735−32.

OH356·64−0·32 (*Fig. 7*). Single weak feature at 1612 MHz. Slightly stronger emission is present at 1667 and 1665 MHz but nothing was detected at 1720 MHz. Also associated is an H_2O maser (Batchelor *et al.* 1980). The masers apparently coincide with IRC−30308 (at R.A. $17^h 35^m 27^s$, Dec. $-31° 55'·8$) and suggest that the object may be an OH/IR late-type star although the 1612 MHz emission shows only one peak and main-line OH emission is unusually strong.

OH357·0+0·0. Type IIc with accompanying 1720 MHz absorption.

OH358·16+0·50 (*Fig. 8*). OH/IR star, CRL 1992; the OH maser was first detected while investigating the IR source (Allen *et al.* 1977).

OH358·67−0·04 (*Fig. 8*). OH/IR star with very wide separation of velocity peaks ($\sim 60\ \mathrm{km\,s^{-1}}$). The OH source may be identified with IRC−30316 but improved position measurements are required to verify this.

OH359·22+0·26. Single feature, source type not known: neither emission nor absorption detected either at 1720 MHz ($<0·2$ Jy) or at 1665 MHz ($<0·5$ Jy).

OH1·48−0·06 (*Fig. 9*). This OH source is probably responsible for the 1612 MHz OH emission found by Dickinson and Chaisson (1974) when they searched for OH in the direction of the far-IR object Hoffmann 37. However, Dickinson and Chaisson detected only the feature at $-114\ \mathrm{km\,s^{-1}}$ owing to their limited search range in velocity. Their intensity of 40 Jy is ~ 4 times greater than ours and at face value suggests gross variability, which merits further investigation. The Hoffmann IR source has a large uncertainty in position ($\sim 6'$ arc), and thus it is not clear whether it is related to the OH maser (despite its role in motivating the search by Dickinson and Chaisson).

Figs 1–9. OH emission sources at 1612 MHz. The total intensity (sum of two circular polarizations) is plotted as a function of radial velocity relative to the local standard of rest. See Table 1 for observation dates.

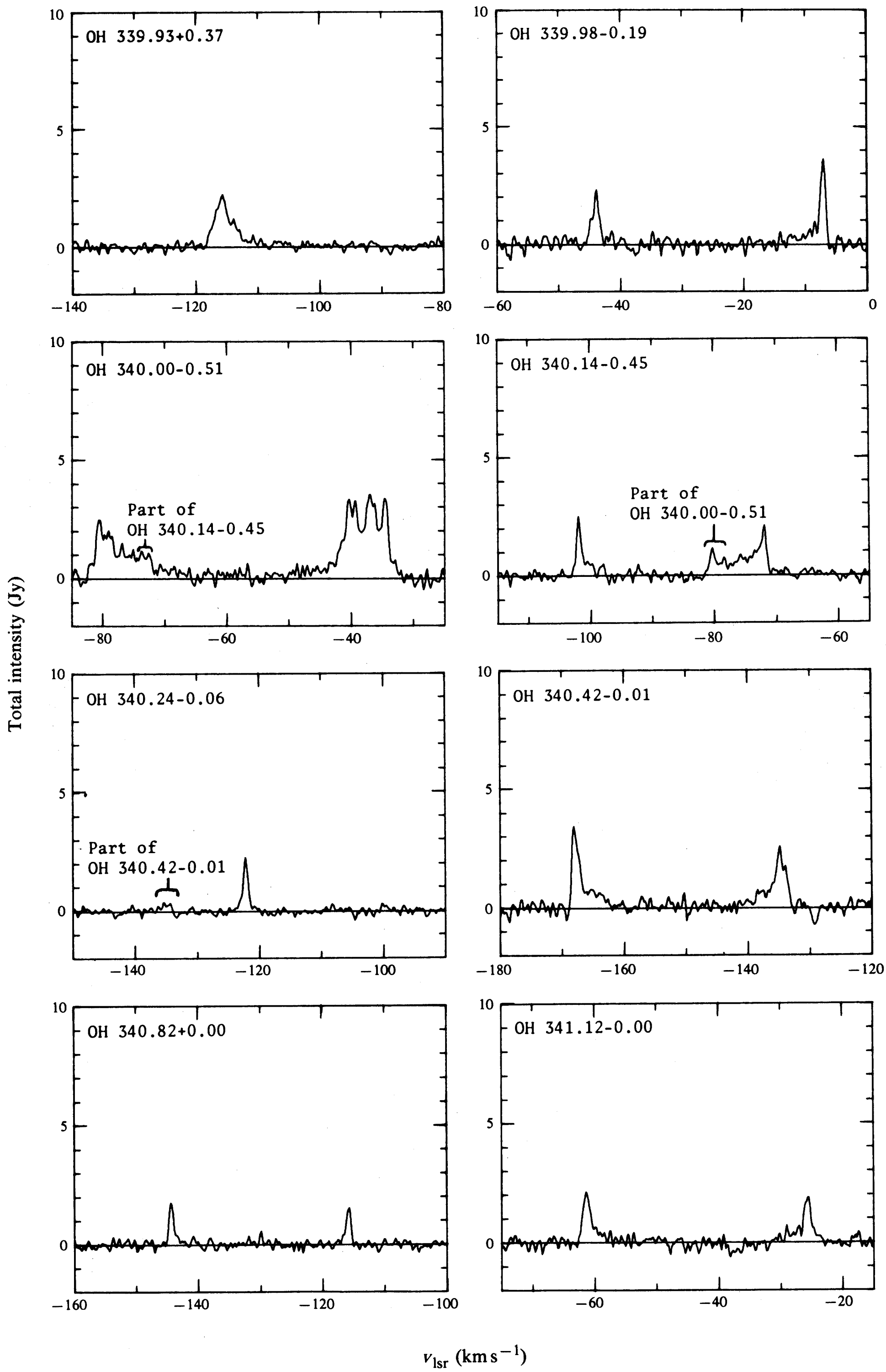
OH 339.93+0.37
OH 339.98-0.19
OH 340.00-0.51
Part of
OH 340.14-0.45
OH 340.14-0.45
Part of
OH 340.00-0.51
OH 340.24-0.06
Part of
OH 340.42-0.01
OH 340.42-0.01
OH 340.82+0.00
OH 341.12-0.00
Total intensity (Jy)
v_{lsr} (km s^{-1})

Fig. 1

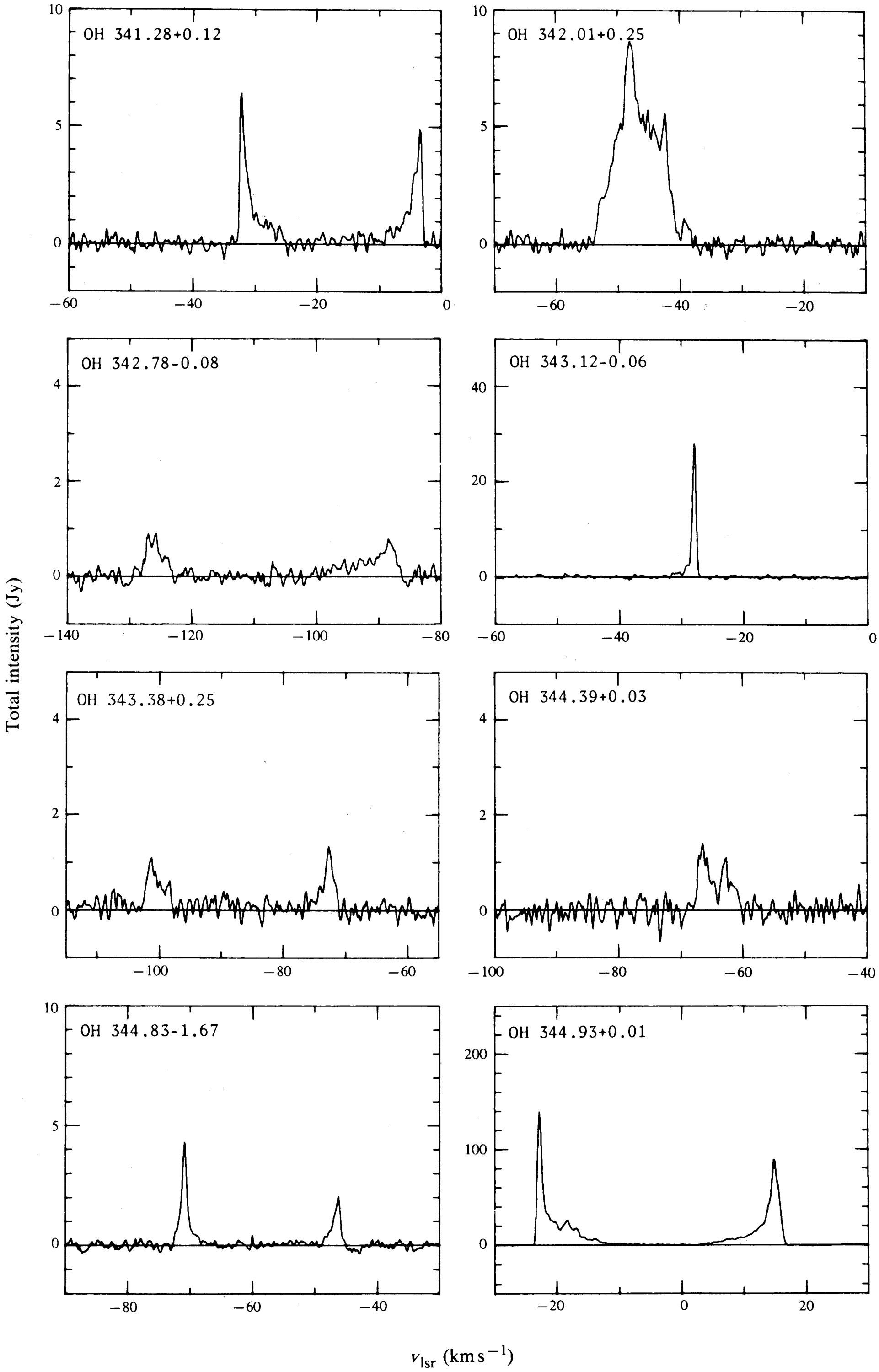
OH 341.28+0.12
OH 342.01+0.25
OH 342.78-0.08
OH 343.12-0.06
OH 343.38+0.25
OH 344.39+0.03
OH 344.83-1.67
OH 344.93+0.01
Total intensity (Jy)
v_{lsr} (km s^{-1})

Fig. 2

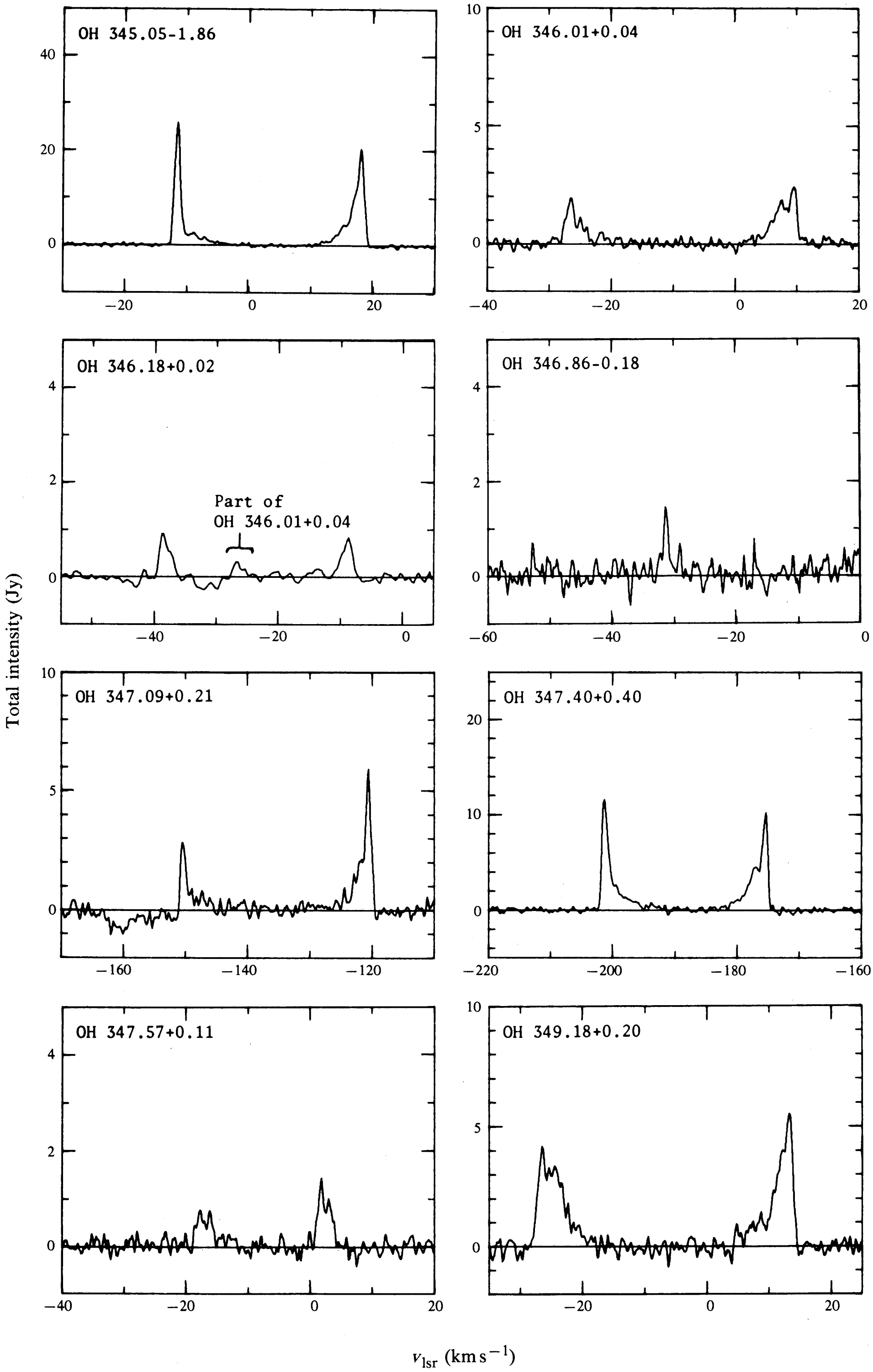
OH 345.05-1.86
OH 346.01+0.04
OH 346.18+0.02
Part of
OH 346.01+0.04
OH 346.86-0.18
OH 347.09+0.21
OH 347.40+0.40
OH 347.57+0.11
OH 349.18+0.20
Total intensity (Jy)
v_{lsr} (km s^{-1})

Fig. 3

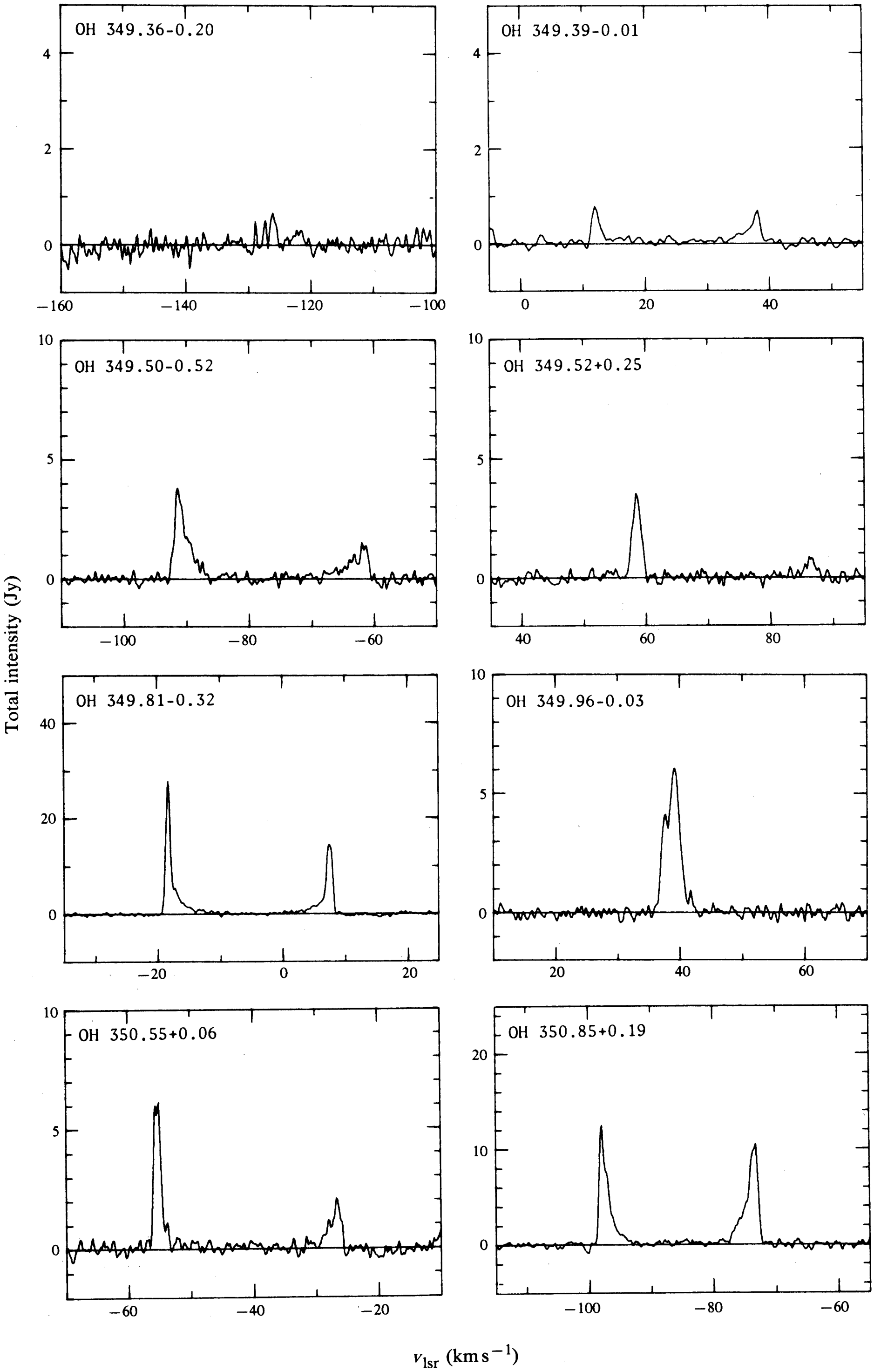

OH 349.36-0.20
OH 349.39-0.01
OH 349.50-0.52
OH 349.52+0.25
OH 349.81-0.32
OH 349.96-0.03
OH 350.55+0.06
OH 350.85+0.19
Total intensity (Jy)
v_{lsr} (km s^{-1})

Fig. 4

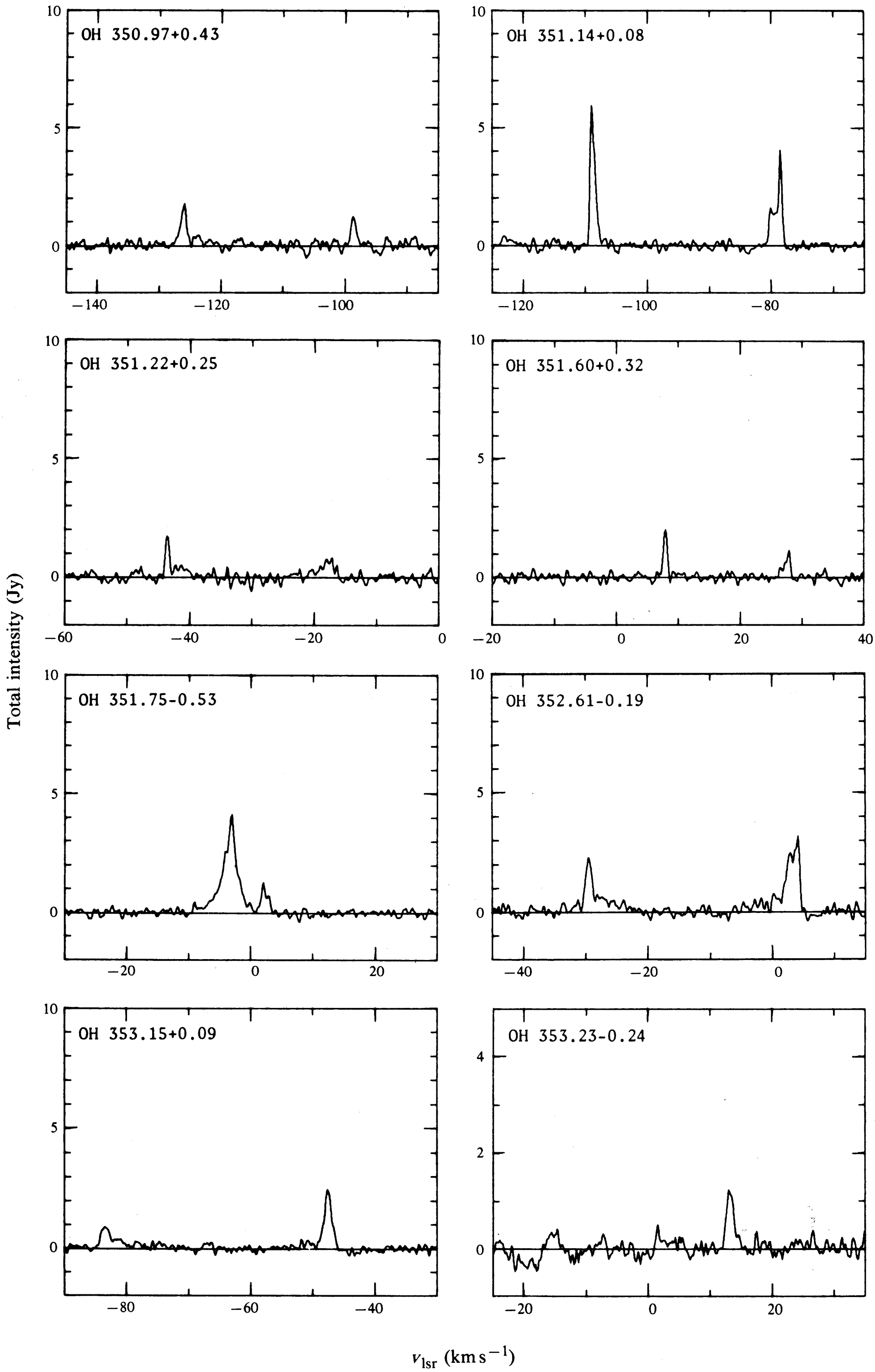
OH 350.97+0.43
OH 351.14+0.08
OH 351.22+0.25
OH 351.60+0.32
OH 351.75-0.53
OH 352.61-0.19
OH 353.15+0.09
OH 353.23-0.24
Total intensity (Jy)
v_{lsr} (km s^{-1})

Fig. 5

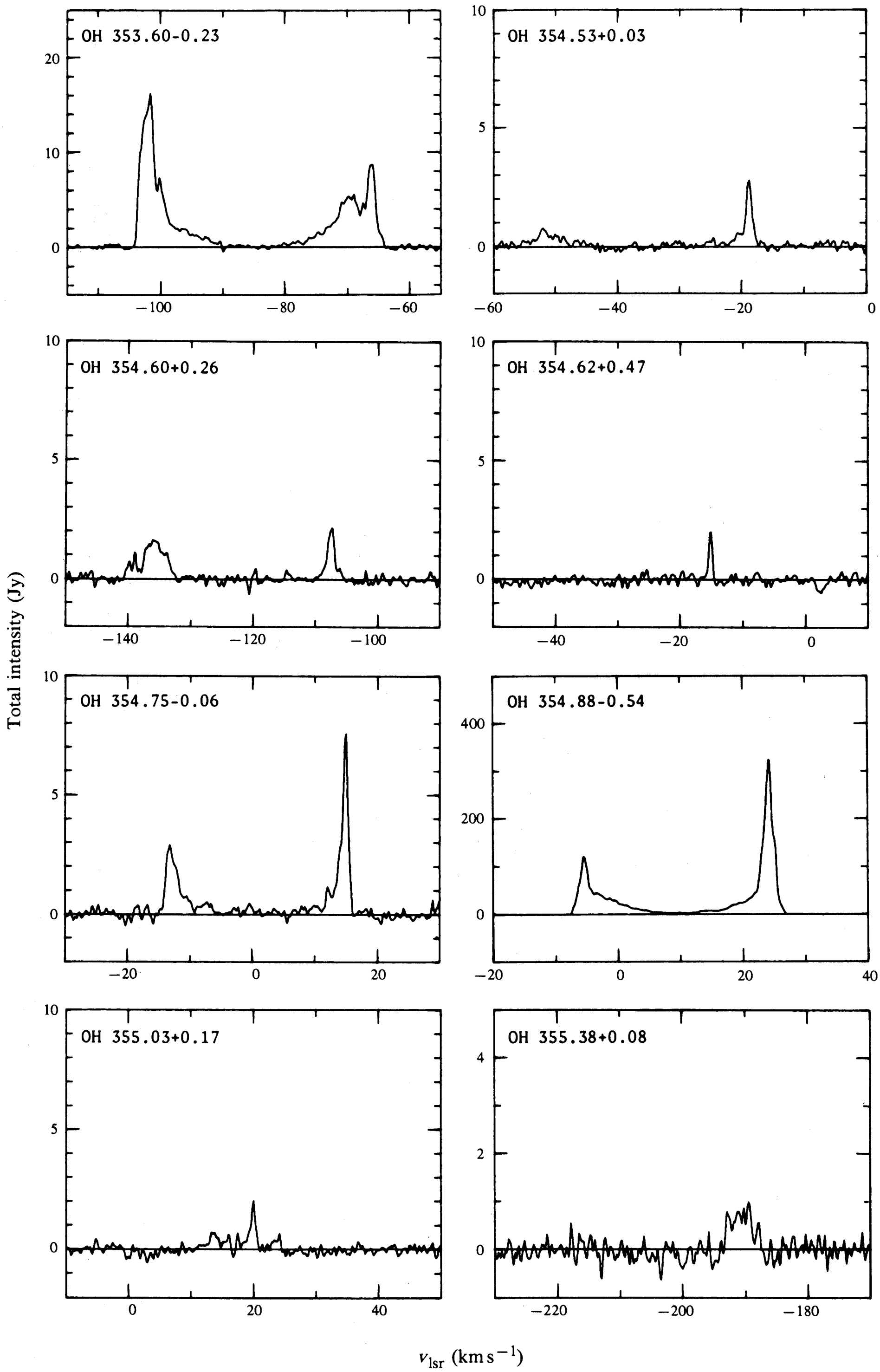
OH 353.60-0.23
OH 354.53+0.03
OH 354.60+0.26
OH 354.62+0.47
OH 354.75-0.06
OH 354.88-0.54
OH 355.03+0.17
OH 355.38+0.08
Total intensity (Jy)
v_{lsr} (km s^{-1})

Fig. 6

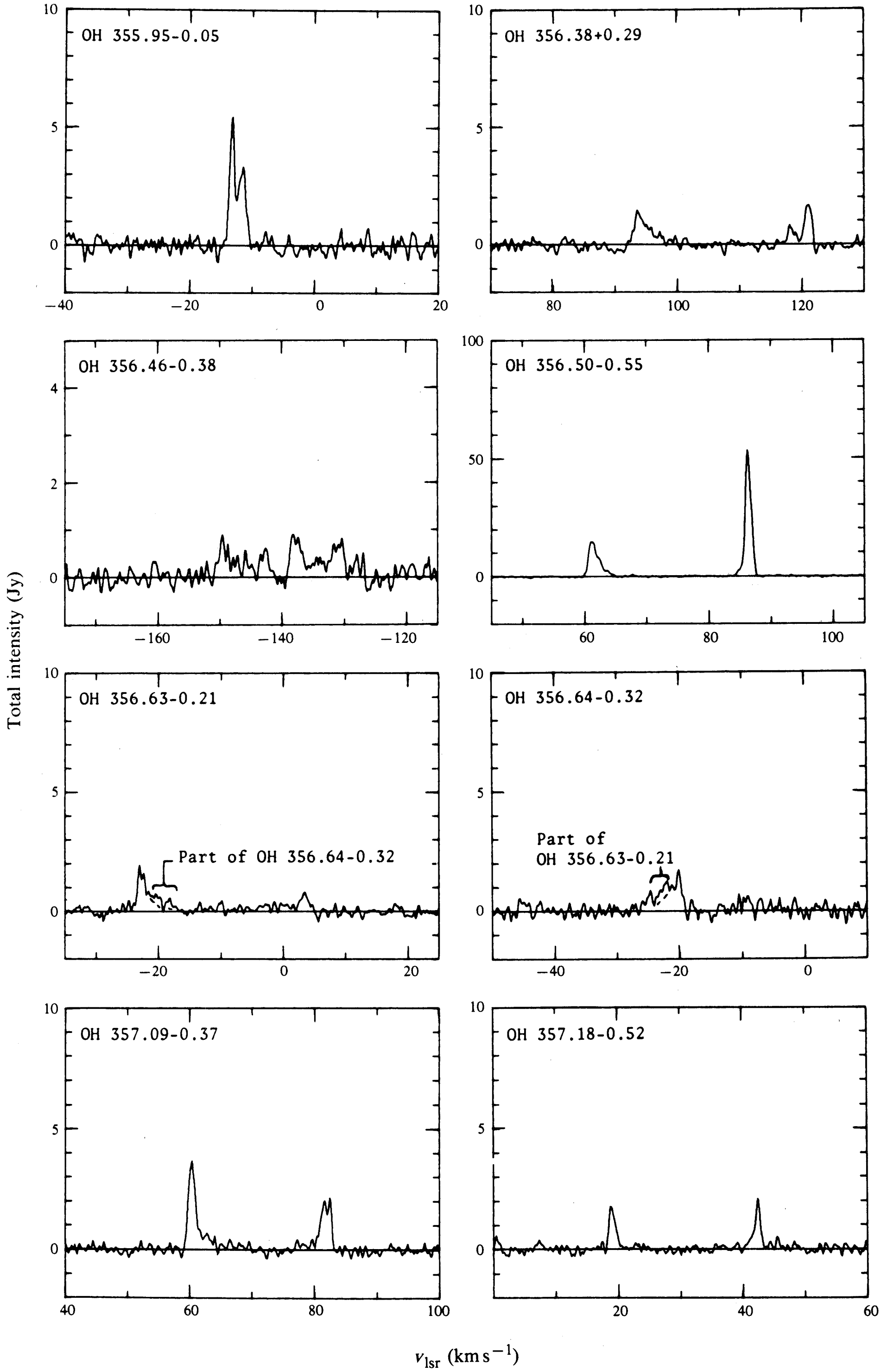
OH 355.95-0.05
OH 356.38+0.29
OH 356.46-0.38
OH 356.50-0.55
OH 356.63-0.21
Part of OH 356.64-0.32
OH 356.64-0.32
Part of
OH 356.63-0.21
OH 357.09-0.37
OH 357.18-0.52
Total intensity (Jy)
v_{lsr} (km s^{-1})

Fig. 7

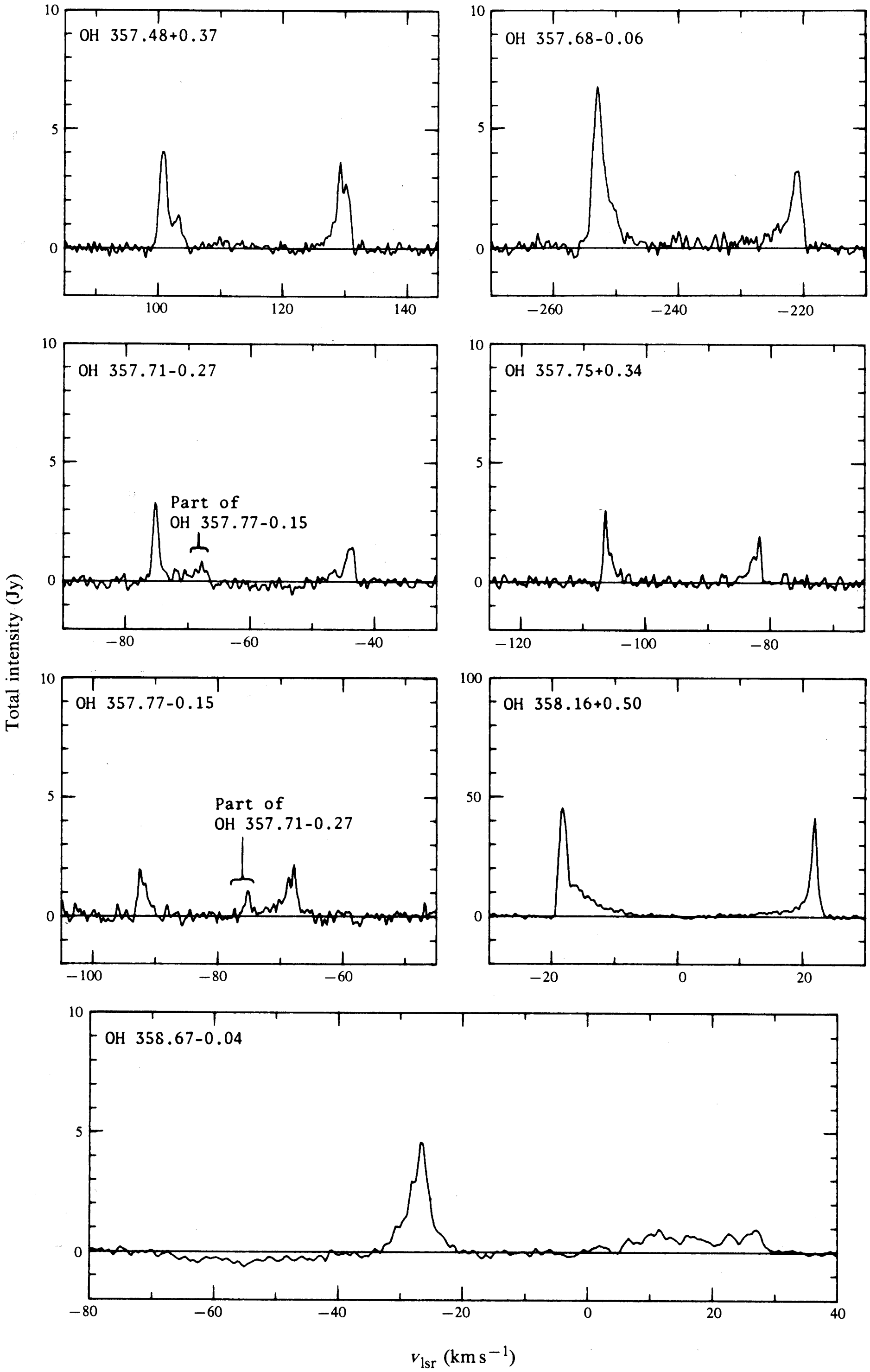
OH 357.48+0.37
OH 357.68-0.06
OH 357.71-0.27
Part of
OH 357.77-0.15
OH 357.75+0.34
OH 357.77-0.15
Part of
OH 357.71-0.27
OH 358.16+0.50
OH 358.67-0.04
Total intensity (Jy)
v_{lsr} (km s^{-1})

Fig. 8

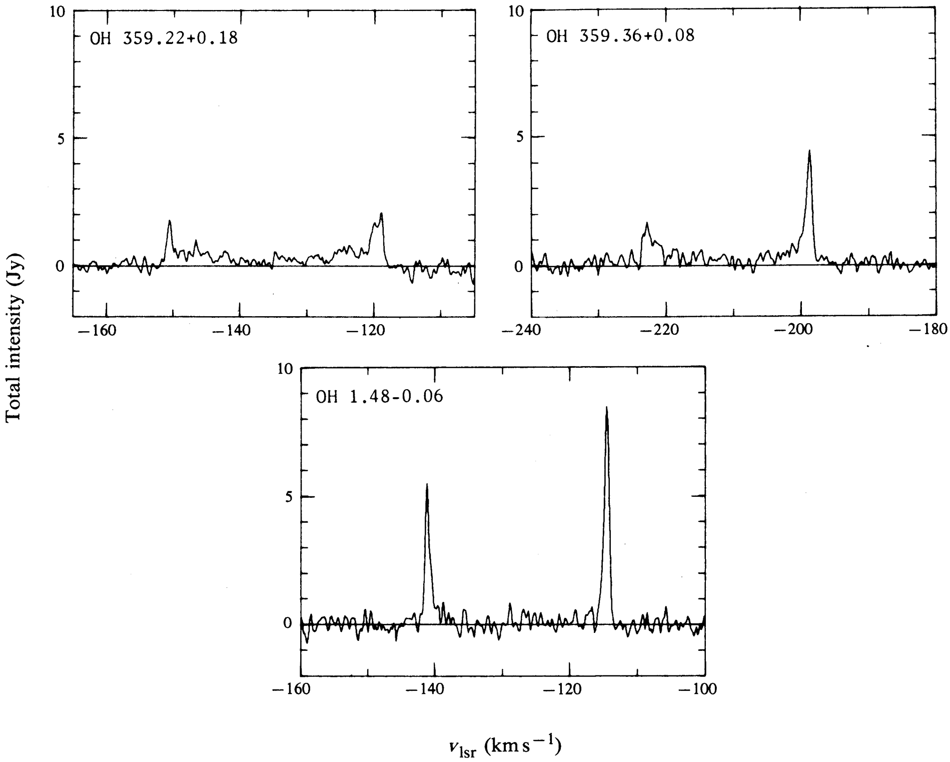

Fig. 9

4. Discussion of the 50 OH/IR Unidentified Stars in the Longitude Range 340° to the Galactic Centre

(*a*) *Velocities and Longitude Distribution*

According to the expanding shell model (see e.g. Caswell 1974) the *mean* velocity v of the two OH peaks is the systemic velocity; the velocity *separation* of the steep outer edges of the profile is probably the best measure of twice the expansion velocity, but to retain uniformity with earlier work we tabulate the slightly smaller value, the separation of the *peaks* Δv.

The velocity separations range from 19 to 53 km s^{-1} and a histogram showing the distribution is given in Fig. 10. This is essentially the same as that found in surveys covering other ranges of longitude. While it is commonly believed that the distribution may comprise two overlapping populations, with Mira variables accounting for the sources with small Δv and supergiants accounting for those with large Δv, these cannot be distinguished without the aid of additional measurements, for example in the IR.

The line-of-sight component of the systemic velocity of a source can yield a distance estimate if the motion of the source is controlled principally by galactic rotation (e.g. as approximated by Schmidt's (1965) model). Near $l = 0$ such kinematic distances r generally have large uncertainties, since dv/dr is small and a source with $v \approx 0$ may be at any distance up to the far edge of the Galaxy ($\sim$25 kpc). However, in the present survey of the longitude range 340°–360° very few of the sources have v near zero and we will now show that the bulk of them must be quite close to (within $\sim$4 kpc of) the galactic centre—where large peculiar motions are common.

Consider first the sources with quite large *negative* radial velocities: these are probably near the galactic centre, as indicated directly from the rotation model; objects with large *positive* velocities are also likely to be near the galactic centre (rather than local), since such velocities in OH/IR stars are rare at $l < 340°$ (cf.

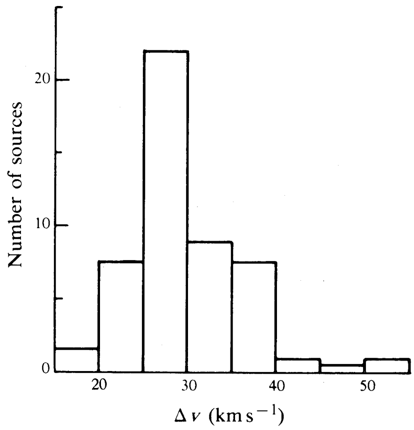

Fig. 10. Histogram of the velocity separations of the peaks Δv for OH/IR stars in the longitude range 340° to the galactic centre.

Caswell and Haynes 1975) and the density of *local* objects would show no such sharp dependence on longitude. There remain the sources with velocities near zero: on the assumption of strict circular rotation a formal solution indicates that these may either be local or at $\sim$20 kpc (twice the galactic centre distance); because our survey is sensitivity-limited many more objects are likely to be local than at very large distances so the local distance is preferred, especially in those instances where the source is of above average intensity. However, it is possible that in some instances even these low velocity sources may be near the galactic centre.

With the preceding arguments in mind we have estimated the kinematic distances. For quite large negative velocities where the calculated distance turns out to be within 4 kpc of the galactic centre, we quote the distance of the tangential point with the 'near' and 'far' solutions as upper and lower limits (or the tangential point distance alone if the velocity is 'forbidden'). For large positive velocities (>20 km s^{-1}), again we quote the tangential point distance. For small velocities where the calculated position is located more than 4 kpc from the galactic centre, the preferred distance is the nearby one but a location near the galactic centre is possible and in a few cases even the far distance ($\sim$20 kpc) may be the correct one. Preferred distances are printed in italics in Table 1, column 13. It can be seen from Table 1 that for more than half the sources the preferred distance lies within 4 kpc of the galactic centre and has a typical uncertainty of less than a factor of 2.

Following their discovery of an OH/IR star with velocity of -342 km s^{-1}, Baud *et al.* (1975) suggested that many high velocity OH/IR stars might be present near the galactic centre; however, in our survey the highest velocity detected was -237 km s^{-1} (for OH 357·68$-$0·06) and for only one other source did $|v|$ exceed 200 km s^{-1}. In Fig. 11 we show the distribution of velocities of OH/IR sources from the present survey, together with sources in the longitude range 326°–340° from Caswell and Haynes (1975) and sources with $l < 90°$ from Johansson *et al.*

(1977*a*), Bowers (1978*a*) and Baud *et al.* (1979*a*, 1979*b*). However, we have omitted all sources with $|b| > 0°\cdot 6$ (these comprise slightly less than half of the known northern sources): our reason for this is that, in the southern sky, latitudes larger than $0°\cdot 6$ have not been searched and thus our restriction of the northern sample to this same narrow range of $|b|$ makes it more nearly homogeneous with the southern search. Furthermore, Habing (1977) pointed out that at large values of $|b|$ there seems to be an increased proportion of very high velocity sources and the exclusion of sources at large $|b|$ on *both* sides of the galactic centre is desirable to prevent any spurious asymmetry about the centre.

In general, Fig. 11 shows an approximate antisymmetry about the galactic centre, as expected from the effects of galactic rotation; it is of particular interest to ascertain whether there are any significant departures from this antisymmetry. Bowers (1978*b*) suggested that l–v data for $l > 12°$ indicated a concentration of sources at the position of the expanding 4 kpc ring, with a deficiency closer to the galactic centre. Additional data from Baud *et al.* (1979*a*, 1979*b*) and the present survey do not support this deficiency, but the possible influence of the expanding 4 kpc arm may be manifested by the following. There is a marginal indication that, near $l = 0$, negative velocities predominate: 12 out of 17 sources with l between 0° and 5° have negative velocities, with the mean value being $-22\ \mathrm{km\,s^{-1}}$; 8 out of 15 sources with l between 355° and 0° have negative velocities, the mean value being $-30\ \mathrm{km\,s^{-1}}$. Sources on the near side of the expanding arm tend to have negative velocities and, because of the survey sensitivity limits, sources on the near side predominate over those on the far side; this could account for the observed preponderance of negative velocities at *both* $l > 0°$ and $l < 0°$.

Apart from the region with $|l| < 5°$, Fig. 11 confirms an approximate antisymmetry between positive and negative longitudes: between longitude 326° and 355°, 5 of the 48 sources have positive velocities and 6 sources exceed the maximum 'allowed' negative velocity; between longitudes 5° and 34°, 7 of the 55 sources have negative velocities and 7 exceed the maximum 'allowed' positive velocity.

If we disregard the velocities, the longitude distribution shows a falloff in sources for $l > 35°$, from which both Johansson *et al.* (1977*b*) and Bowers (1978*b*) inferred that the numbers of OH/IR stars are dropping quite rapidly beyond 6 kpc from the galactic centre. Bowers (1978*b*) further concluded that the numbers also fall off toward the galactic centre, while Baud (1978) suggested that there was a secondary increase close to the galactic centre. With the improved statistics resulting from coverage both sides of the galactic centre, it now appears that there is indeed a maximum within 1 kpc (5°) of the galactic centre followed by a slow falloff; a marginally significant secondary maximum occurs at ~5 kpc from the centre (i.e. at $|l| \approx 23°$) and then there is a quite marked decrease in source density.

(*b*) *Luminosity Function*

Using the peak flux density multiplied by the square of the distance as a luminosity measure (column 14 of Table 1) we plot a histogram of the observed luminosity function in Fig. 12. Because many sources are near the galactic centre, there is no doubt that typical luminosities as large as several hundred $\mathrm{Jy\,kpc^2}$ are common among OH/IR stars, as was pointed out by Caswell and Haynes (1975). However, the luminosity of some of the apparently strongest sources might be overestimated

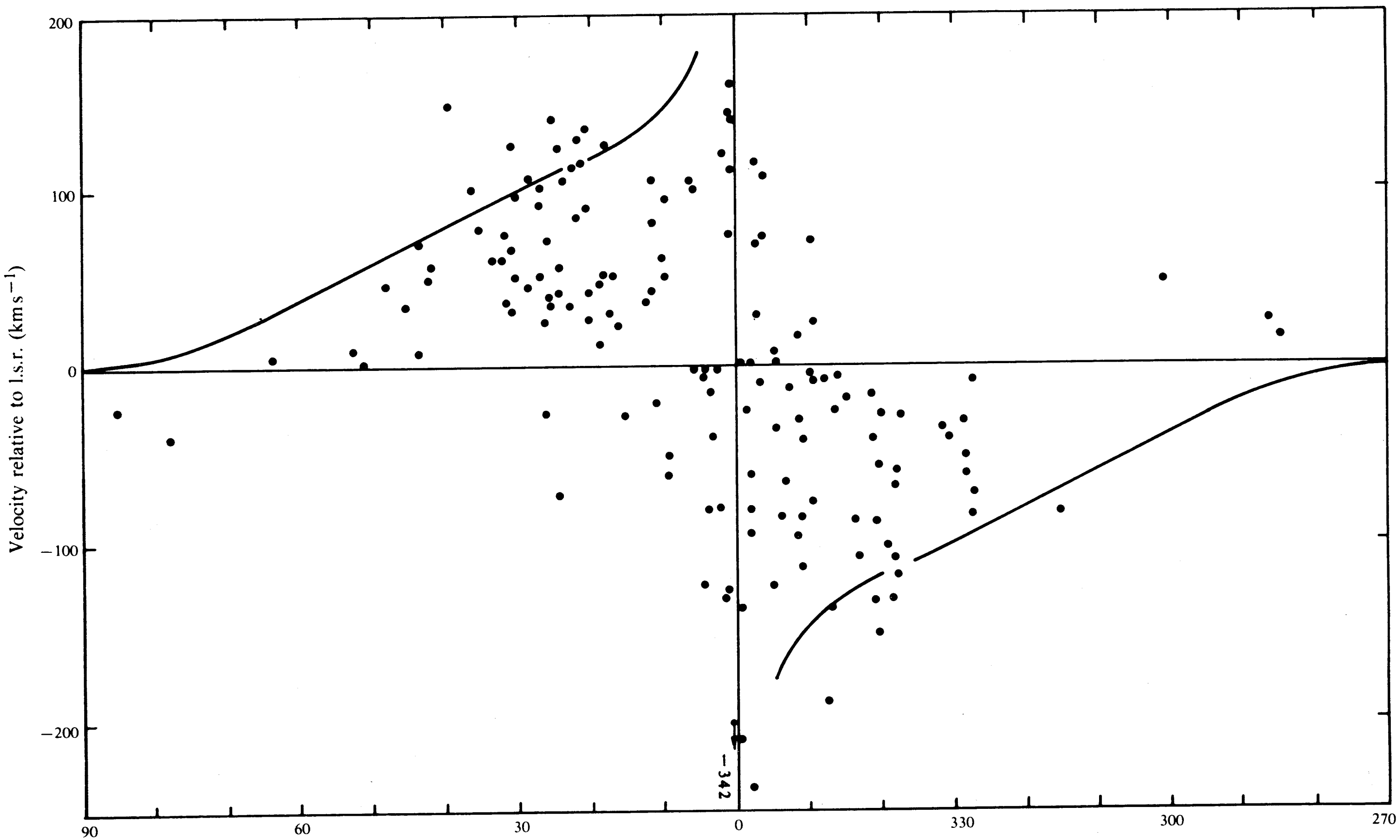

Fig. 11. Distribution of mean velocities for OH/IR stars at low galactic latitude ($|b| < 0°\cdot6$) and with galactic longitude within 90° of the galactic centre. The curves show the maximum 'allowed' velocity on the assumption of strict circular motion defined by Schmidt's (1965) galactic rotation model.

by a factor of ~ 3 if they are on the near side of the '4 kpc arm' rather than at the galactic centre. Any attempt at constructing the true luminosity function should allow for the strong effects of the survey sensitivity limit at low luminosity. If allowance for this is made, the low luminosity cutoff is not real, as was pointed out by Baud (1978) from his northern hemisphere data. Indeed, the known Mira variables represent a large population with OH emission of lower luminosity than the sources studied here; however, it is not clear whether the bulk of the unidentified sources represent a high luminosity tail of the Miras or are a distinct, unrelated, population. Classification of the individual sources by their IR and other properties is needed to clarify this matter (see Section 7 below).

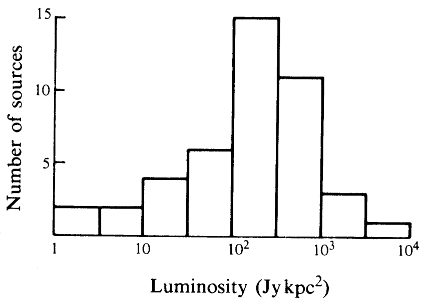

Fig. 12. Observed histogram of luminosities for OH/IR stars observed in the present survey. Luminosity is measured as the product of the peak flux density and the square of the distance.

5. The Type I Sources

Four of the quite strong 1612 MHz masers appear to be intimately associated with type I (main-line) emission; such 1612 MHz emission is not uncommon and occurs in about 15% of type I masers (cf. Caswell *et al.* 1980).

The longitude range 340°–360° is being searched thoroughly for main-line emission (as was done for longitudes 326°–340° by Caswell *et al.* 1980); preliminary results cited earlier in the notes in Section 3*b* have been referenced as Caswell and Haynes (unpublished data) and we will discuss the type I sources in more detail when the survey is complete.

6. Comparison with the Previous Parkes 1612 MHz Survey

In the 1612 MHz survey of the longitude range 326°–340° (Caswell and Haynes 1975), 27 sources were detected; of these, 15 were OH/IR stars, 7 were type IIc, 4 were type I and 1 was a single feature, type unknown. In the present survey of longitude range $\sim 340°$ to the galactic centre, out of 77 sources detected, 49 were OH/IR stars, 11 were type IIc, 4 were type I and 13 were single features which could not readily be classified. Proportionately the present survey shows an excess of OH/IR stars, and this is probably attributable to their increased density close to the galactic centre. But perhaps the most striking aspect is the presence of a large number of unclassifiable sources; these clearly require further study, since some may be truly unusual sources while others are probably OH/IR stars in which the second feature is below present detection limits.

7. Conclusions

Historically the double-peaked 1612 MHz OH masers studied here have been dubbed 'unidentified OH/IR stars'—but of course the 'unidentified' designation describes an accidental (and sometimes short-lived) 'property' rather than being a strict definition (in particular the southern OH sources have been detected prior to any comprehensive IR survey and thus are nearly all unidentified). As it turns out, the sample of such sources is almost unchanged if it is defined by a sensitivity limit *in the OH emission* together with a small galactic latitude limit (these limits exclude almost all of the low-luminosity nearby identified stars). The complete radio sample now needs complementary IR measurements; ultimately it may be expected that all sources will be identified and the objects will then achieve their full potential as valuable stellar probes extending to the innermost regions of the Galaxy, with no selection effects imposed by optical obscuration. Speculations on the relative proportions of Mira variables, late-type supergiants and any possible additional class (e.g. by Johansson *et al.* 1977*b*; Bowers 1978*b*; Baud 1978) are still inconclusive and will be best resolved by observations in the IR and by monitoring both the OH and IR emission for variability. For the more powerful objects, interferometry to determine the spatial structure of the OH emission will improve our understanding of the circumstellar cloud geometry, since current models rely heavily on the only well-observed sources, NML Cyg and VY CMa (Benson and Mutel 1979).

Acknowledgment

One of us (U.M.) thanks CSIRO for a research fellowship and generous hospitality during his leave of absence from Bonn.

References

Allen, D. A., Hyland, A. R., Longmore, A. J., Caswell, J. L., Goss, W. M., and Haynes, R. F. (1977). *Astrophys. J.* **217**, 108.

Batchelor, R. A., Caswell, J. L., Goss, W. M., Haynes, R. F., Knowles, S. H., and Wellington, K. J. (1980). *Aust. J. Phys.* **33**, 139.

Baud, B. (1978). Ph.D. Dissertation, University of Leiden.

Baud, B., Habing, H. J., Matthews, H. E., O'Sullivan, J. D., and Winnberg, A. (1975). *Nature* **258**, 406.

Baud, B., Habing, H. J., Matthews, H. E., and Winnberg, A. (1979*a*). *Astron. Astrophys. Suppl.* **35**, 179.

Baud, B., Habing, H. J., Matthews, H. E., and Winnberg, A. (1979*b*). *Astron. Astrophys. Suppl.* **36**, 193.

Benson, J. M., and Mutel, R. L. (1979). *Astrophys. J.* **233**, 119.

Bowers, P. F. (1978*a*). *Astron. Astrophys. Suppl.* **31**, 127.

Bowers, P. F. (1978*b*). *Astron. Astrophys.* **64**, 307.

Bowers, P. F., and Kerr, F. J. (1978). *Astron. J.* **83**, 487.

Caswell, J. L. (1974). *In* 'Galactic Radio Astronomy', Proc. IAU Symp. No. 60 (Eds F. J. Kerr and S. C. Simonson III), p. 423 (Reidel: Dordrecht).

Caswell, J. L., and Haynes, R. F. (1975). *Mon. Not. R. Astron. Soc.* **173**, 649.

Caswell, J. L., Haynes, R. F., and Goss, W. M. (1980). *Aust. J. Phys.* **33**, 639.

Caswell, J. L., and Robinson, B. J. (1974). *Aust. J. Phys.* **27**, 629.

Dickinson, D. F., and Chaisson, E. J. (1974). *Astron. J.* **79**, 938.

Habing, H. J. (1977). *In* 'The Interaction of Variable Stars with their Environment', Proc. IAU Colloq. No. 42 (Eds R. Kippenhahn, J. Rabe and W. Strohmeier), Veroeff. der Remeis-Sternwarte Bamberg, Vol. XI, No. 121, p. 401.

Hardebeck, E. G. (1972). *Astrophys. J.* **172**, 583.

Johansson, L. E. B., Andersson, C., Goss, W. M., and Winnberg, A. (1977*a*). *Astron. Astrophys. Suppl.* **28**, 199.

Johansson, L. E. B., Andersson, C., Goss, W. M., and Winnberg, A. (1977*b*). *Astron. Astrophys.* **54**, 323.

Knowles, S. H., Caswell, J. L., and Goss, W. M. (1976). *Mon. Not. R. Astron. Soc.* **175**, 537.

Robinson, B. J., Caswell, J. L., and Goss, W. M. (1974). *Aust. J. Phys.* **27**, 575.

Schmidt, M. (1965). *In* 'Galactic Structure' (Eds A. Blauuw and M. Schmidt), p. 513 (Univ. Chicago Press).

Manuscript received 1 August 1980, accepted 9 December 1980